Original Article

Access this article online
Quick Response Code:

Website: www.carcinogenesis.com
DOI: 10.4103/jcar.jcar_22_02_01

Enhancing the Antibacterial Activity of Synthesized Silver Nanoparticles with Weak Static Magnetic Fields: A Comparative Study on Bacterial Growth Inhibition

Dalya A. Huseen[1], Mazin K. Hamid [1], Mais E. Ahmed [2]

Abstract

The use of silver nanoparticles as a potential solution to the problem of antimicrobial-resistant bacteria is a huge concern with antibiotic resistance, especially multidrug-resistant bacteria. Because antimicrobial-resistant bacteria endanger the security and effectiveness of contemporary medical procedures Antibiotic resistance is used to biosynthesize silver nanoparticles by Pseudomonas aeruginosa. The paper will compare the antibacterial activity of silver nanoparticles synthesized by biological by well diffusion method with and without the effect of the weak static magnetic field. The UV spectrophotometer showed the peak absorption at 421nm wavelength. Transmission electron microscopy(TEM) showed nanoparticles were homogeneous and spherical in shape with an average size of 24.5 nm, energy dispersive X-ray spectroscopy(EDS), confirm the purity of the synthesized nanoparticle Atomic force microscopy(AFM) Showed an average diameter of 56.76 nm, XRD Showed the crystallites with average size36.6nm of the synthesized nanoparticles, zeta potential was fined to be -29.30 mv and field emission scanning electron microscopy(FESEM) Was Find Between (23-24.9)nm. Where it was observed that the best inhibitory the minimum inhibitory concentration was 32 μg/ml concentration and showed the best efficacy against resistant strains of Gram-positive and negative bacteria against multidrug-resistant bacteria, and Study Cytoxocity Assay A549 on the carcinoma cell line.

Keywords:

Silver nanoparticles, A549 cell line, Cytotoxicity, Magnetic fields.

Introduction

Nanotechnology is the creation of materials and devices through the control of matter at the atomic, molecular, and supramolecular (nanoscale) levels. This is the creation of large-scale new materials using very small material particles to better understand the differences between different scales [1]. About 100,000 tons of antibiotics for intended illnesses are generated globally each year. Misuse who is this quantity of antibiotics has led to the emergence of many medicine impedances between disease-causing strains, especially bacteria. Most of these applications benefit from the unique physicochemical properties exhibited by Ag with nanoscale particle sizes [2]. The dimensional properties determine the design and application modes of these nanomaterials [3]. An urgent need to improve the applicability of Ag NPs in new advanced technologies in the field of plasmonic devices and the construction of nano electronic devices [4] and the development of new applications for medical devices and the development of biomedical therapies for related diseases such as certain cancers, viral infections, and pathogens [5].To create a new material with special qualities for numerous technological applications, a variety of magnetic materials were tested in the present study when they were combined to silver-magnetite nanoparticles [6]. The morphology of these extremely crystalline nanoparticles is steady

[1] Department of Physiology and Medical Physics, College of Medicine, Al-Nahrain University/Iraq.
[2]Department of Biology /College of Science / University of Baghdad /Iraq.

Address for correspondence:
Dalya A. Huseen, Department of Physiology and Medical Physics, College 0f Medicine, Al-Nahrain University/Iraq.
E-mail: dalya7160@gmail.com

Submitted: 02-Jan-2023
Revised: 02-Aug-2023
Accepted: 22-Sep-2023
Published: 12-Oct-2023

How to cite this article: Huseen D A, Hamid M K, Ahmed M E. Enhancing the Antibacterial Activity of Synthesized Silver Nanoparticles with Weak Static Magnetic Fields: A Comparative Study on Bacterial Growth Inhibition. J Carcinog 2023;22(2):1-11

and nearly homogeneous. By physical means, static magnetic fields from AgNPs had better antibacterial activity than those from controls [7].

Material and method

Pseudomonas aeruginosa isolated from the burn was cultured in broth and cultured at 37° C. for 24 hours to ban a bacterial supernatant. The bacterial solution was transferred to a tube of 10 ml and centrifuged (6000 rpm, 15 minutes). Transfer the supernatant to another tube and discard the compressed precipitate at the lowest of the tube. [8]

Biosynthesized silver nanoparticles

Much emphasis has been paid to biological processes that produce nanoparticles. Bacteria make silver nanoparticles in an environmentally friendly way [9]. Prepare 100 milliliters of nutrient broth, inoculate a 250 mL

Erlenmeyer flask with Pseudomonas aeruginosa broth medium, incubate the flask containing the medium in an incubator at 37 °C for 1-3 days, then centrifuge broth at 8000 rpm. For 10 min, the cell pellet was discarded and the supernatant was collected for use in silver nanoparticle biosynthesis. The supernatant (100 mL) was placed in a clean 250 mL Erlenmeyer flask, (100 mL) of (1 mM) silver nitrate was added, and the mixture was incubated at 37°C for 48 hrs. Color changes were visually observed and photographed in the dark to avoid AgNO3 oxidation of the biosynthesized SNPs. figure (1)

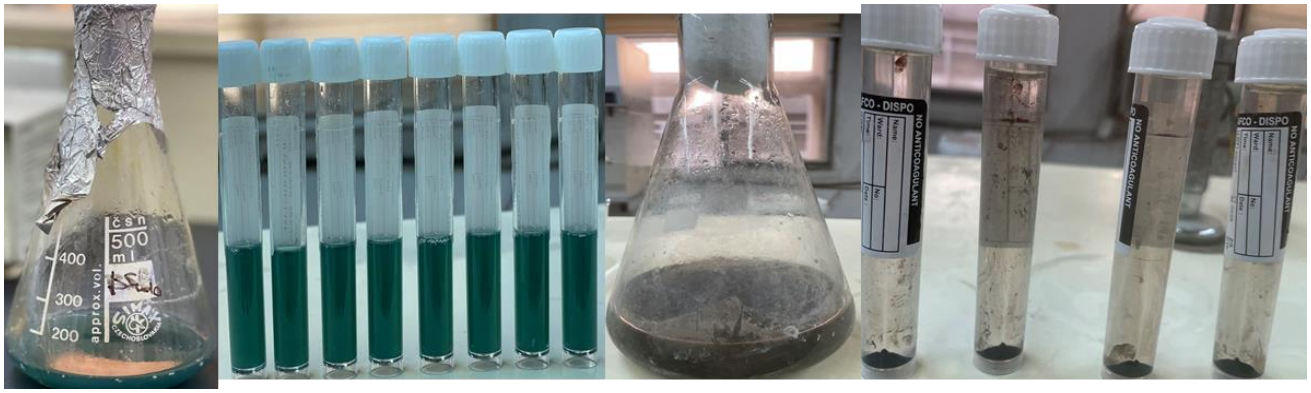

Figure (1): Step of Biosynthesis AgNO3

Static Magnetic field

Neodymium magnets where the permanent magnets were used to produce about 250Mt as shown in figure (2)

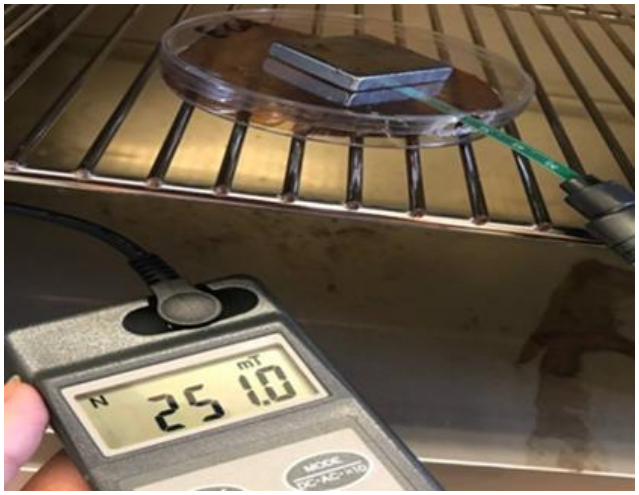

Figure (2): Perment Magnets

Description of biosynthesized AgNPs

Characterization allows for the careful monitoring of shape, size, surface characteristics, and other physiological characteristics. Techniques including X-ray diffraction, transmission electron microscopy, atomic force microscopy, and zeta potential (ZP)[10] are examples of this type of technology. Field ionization Energy dispersive x-ray spectroscopy (EDS) and scanning electron microscopy (FSEM).

UV–Vis Spectrophotometer

A Lambda 45 UV/VIS spectrophotometer was used to search the optical properties of AgNPs. wavelength range from 200 to 700 nm [11]

Analysis of the Zeta Potential

A particle size analyzer was used to measure zeta potential. To lessen the impact of viscosity, samples were properly diluted with room-temperature deionized water[12]

MDR bacteria

Detection of MDR bacteria of gram-negative such as Pseudomonas aeruginosa, and Klebsiella) and gram-positive (S. aureus,_Streptococcus pyogenes) all strain isolation from urine patients suffering wound infection was used to select antibacterial action of AgNPs. There were the lineages acquired microbiology laboratory, at Baghdad University all strain identification by Vitec- 2 system [13].

Minimal inhibitory concentration (MIC):

Different AgNPs extract concentrations (64, 32, 16, 8, 4, and 4) were tested against four strains of bacteria,

including Gram-positive and Gram-negative bacteria, to determine the minimal inhibitory concentration. Tubes were gestated at 37 °C to 24 h using Muller Hinton Broth which contains in each of the 6 tubes. These concentrations were obtained from 0.1 M of metal nanoparticle(MNP). that it has maximum antimicrobial activity within the agar spread examination. later incubating the environment at 37° C. for 24 hours, Observations of the tube's turbidity as an increase and its absence as a rise were made. The minimal sample concentration that represented a clear liquid without turbidity increase was exponentiated as the MIC value. Figure (3)

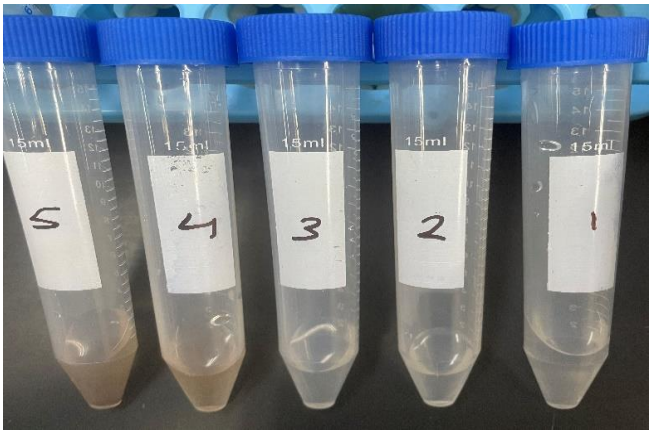

Figure (3): Minimum Inhibitory Concentration of AgNPs (64,32,16,8,4) µg/ml

Well diffusion assay of Antibacterial Activity Without Magnetic Field

Disc diffusion assay was used to quantify antibacterial activity [14, 15]. For each test, overnight MHB cultures of a specific strain of bacteria were freshly made, and inoculations were applied using swabs to the surface of the solidified media. Biosynthesized Ag NPs were impregnated on discs at various concentrations ranging from (64,32,16,8,4) g/ml after the media had dried for 10 minutes.

Well diffusion assay of Antibacterial Activity with Magnetic Field

Disc diffusion assay was used to quantify antibacterial activity [16]. For each test, overnight MHB cultures of a specific strain of bacteria were freshly made, and inoculations were applied using swabs to the surface of the solidified media. After the media had dried for 10 minutes, biosynthesized Ag NPs were impregnated on the discs at the highest concentration determined by a magnetic field-free well diffusion experiment of antibacterial activity; the least inhibitory concentration was 32 g/ml.

Cytotoxic by MTT Assay

Evaluation of the cytotoxic effect of three chemical concentrations of AgNPs on normal HdFn and A375 cells in 96-well plates after 24 hours of AgNPs. To determine the formula, IC50 values: cell viability = Ab S /Ab C — 100 and absorption to 540 nm were measured by usage of Omega micro lamella reader (BMGLABTECH®-FLUO star, Ortenberg, Germany). [17]

Results and discussions

The VITEC-2 system was used to confirm antibiotic susceptibility testing and identification. The classification of all chosen strains as MDR. -lactam antibiotics, microorganism's resistant to cephalosporin

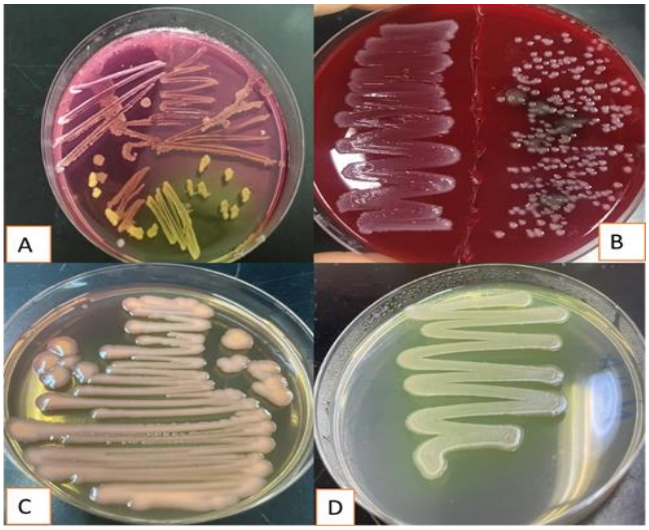

Figure (4): Bacteria isolation A*) S. aureus B) Streptococcus pyogenes C) Klebsiella spp D) Pseudomonas aeruginos*

Biosynthesis of AgNPs

By altering the color of the AgNPs biosynthetic interaction, we see an indication that the formation of AgNPs from a mixture of AgNO3 was monitored using the microbial supernatant during the biosynthetic process. as shown in Figure (5). The color change from white to brownish in the existence of Pseudomonas aeruginosa supernatant is contrasting, no color change in control medium did not influence the decreases of Ag + ions

Figure (5): Powder synthesis of AgNPs

UV–Vis Spectral Analysis:

UV-Vis spectrophotometry was a step toward

characterizing the biosynthesized AgNPs. As a result, it was confirmed that the biosynthesized AgNP has a maximum peak at (421 nm) nm [18]. It is shown in the figure (6). The results are consistent with A.B. Abeer Mohammed. et al [19] when the biosynthetic process of Ag NPs using Pseudomonas aeruginosa supernatant peaks at 300–400 nm using UV-Vis measurements.

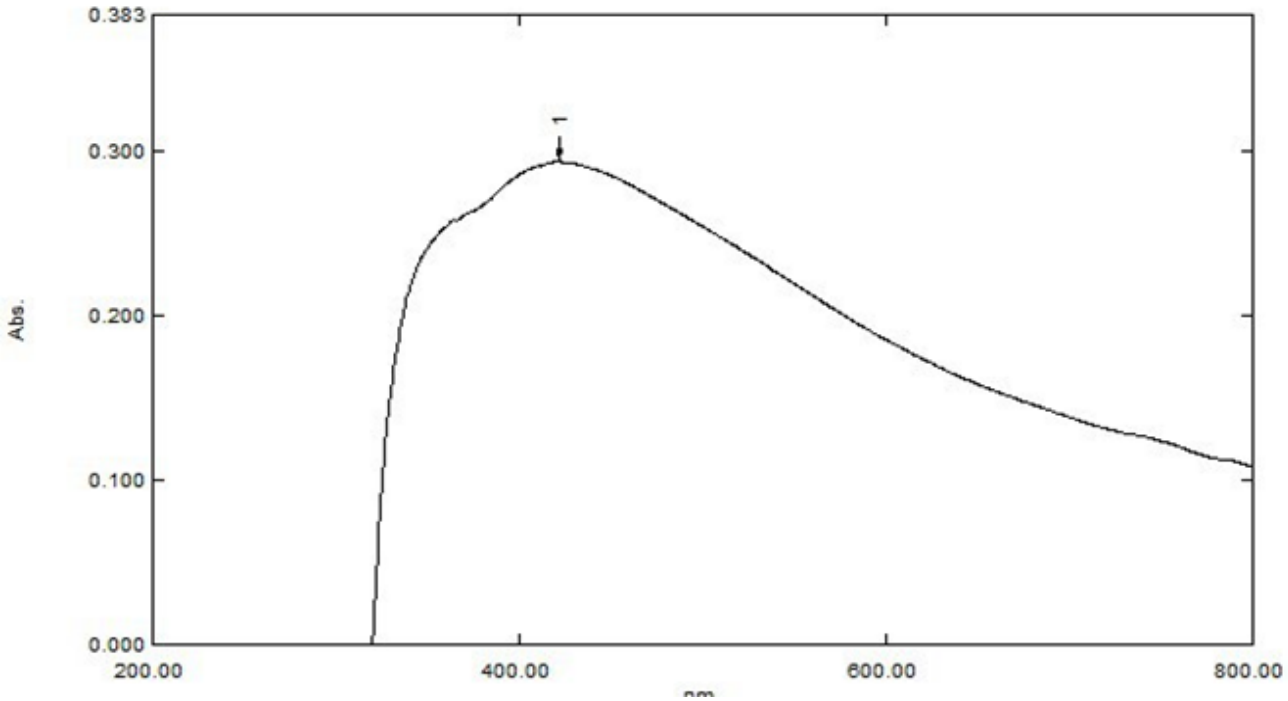

Figure (6): UV–Vis spectrophotometry of Ag NPs Biosynthesized

X-ray Diffraction (XRD)

The XRD spectrum of the Ag nanoparticle powder is recorded in figure (7), and the detection of eminent peaks corresponding to the diffraction peaks of Ag-NPS"(27, 93), (32,35), (46, 34), (54,93), (57.57), (67.54), (74.56), (76.83). Were confirmed. Crystal structures of biosynthetic AgNPs by standard and by using Debay Scherrer equation(D=Kʎ/β$cos\theta$) have been found the nanoparticle size which equals about 36.6nm. agree with[20] the value 2θvalues between 20° and 82° confirmed the Crystal structures of the biosynthesized Ag NPs according standard spectrum

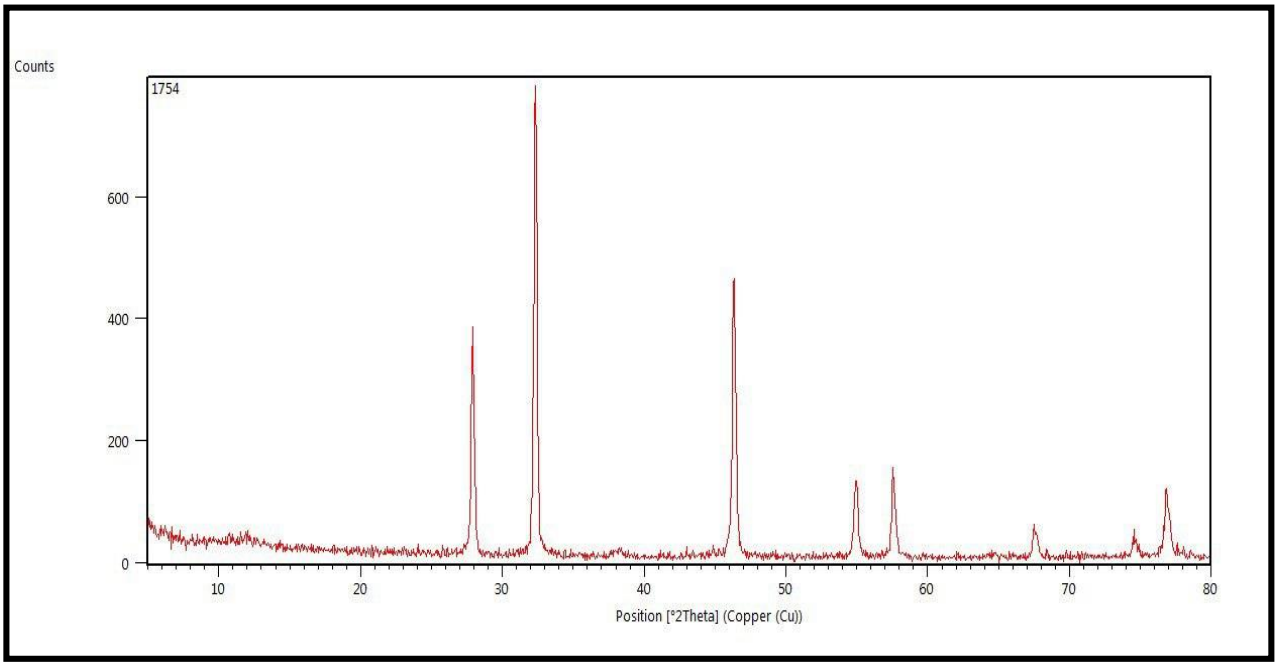

Figure (7): XRD analysis of synthesized Ag NPs

(AFM) analysis

Atomic force microscopy was used as a confirmatory technique to characterize the biosynthesis of AgNPs by determining their 2D and 3D morphologies as well as their average diameters [21]. The results obtained in this study confirmed that the AgNPs biosynthesized via Pseudomonas aeruginosa had an average diameter of 56.76 nm as shown in Figure (8) other study biosynthesis indicated that the diameter of the biosynthesized reached AgNPs 37–168 nm.

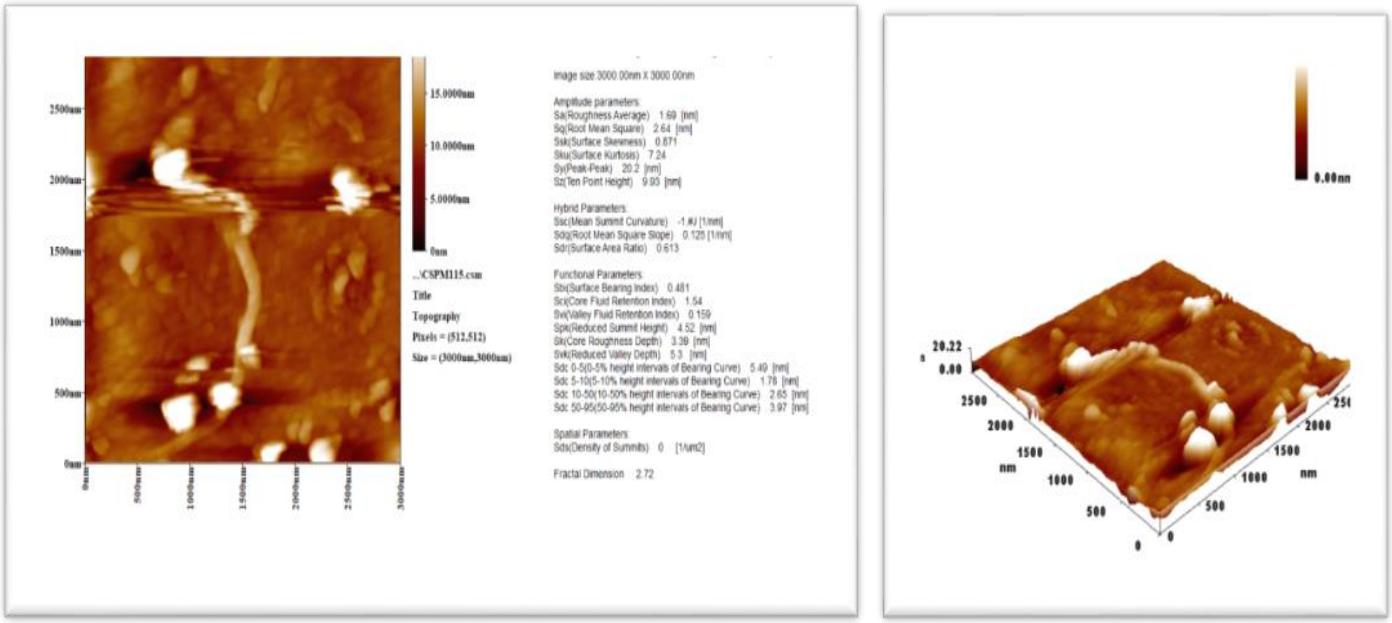

Figure (8): Particle size distribution of biosynthesized AgNPs (A) 2D-AFM of AgNPs (B) 3D-AFM of AgNPs and diagram of AgN

Transmission Electron Microscopy analysis (TEM) of Ag NPs

The TEM micrograph of Ag-NPS was spherical in shape as shown in Figure (9). The nanoparticle diameter was measured to be (24.5-30) nm. These findings are in line with the information provided by Wad Huani et al. in the same context [22].

He concurs that after 168 hours, polydisperse AgNPs from 1 mM AgNO3 with diameters between 10 and 60 nm were discovered by his TEM study [23].

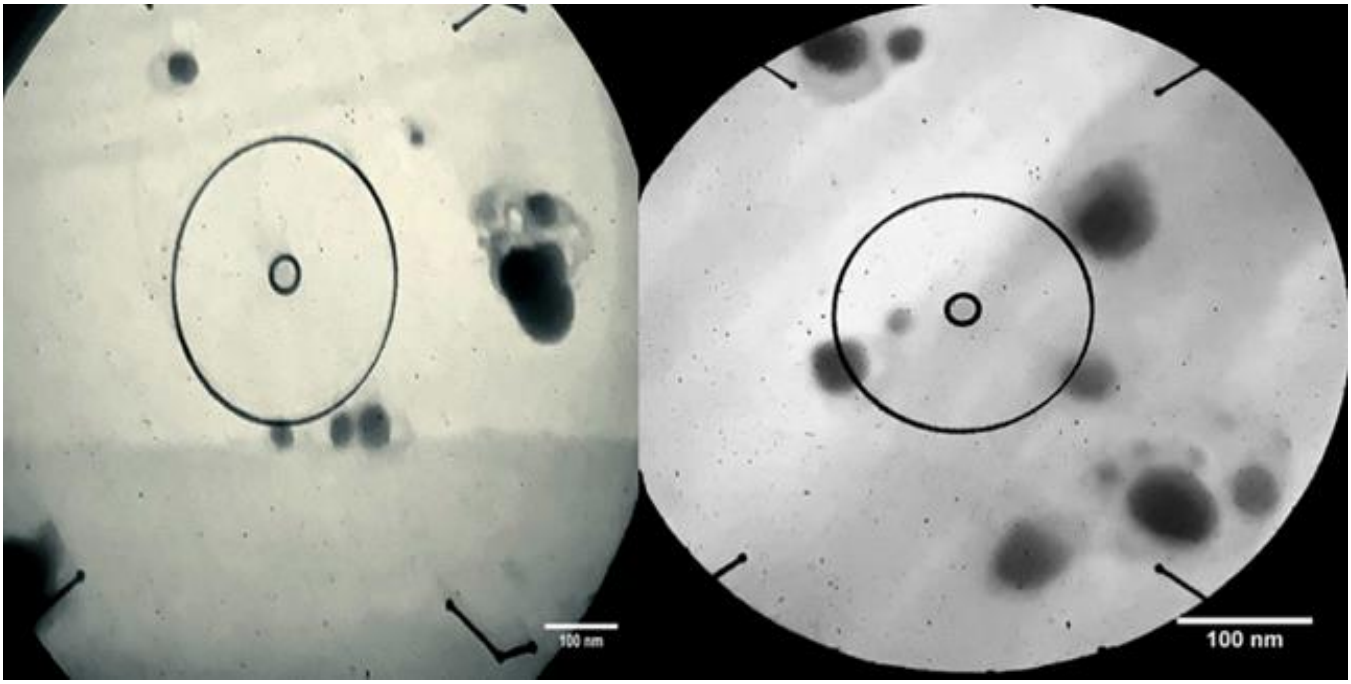

Figure (9): TEM Images of polydisperse AgNPs

Energy dispersive X-Ray spectrometry (EDS) Of AgNPs

(EDS) search endorsed the primary compositions. And the output result of this technique is shown in the figure (10).

The distribution of AgNPs was detected and mapped using EDS [24], and the EDS pattern with a sharp peak at 3 keV, which was characteristic of crystalline metallic silver due to SPR, was supported by the primary compositions [25].

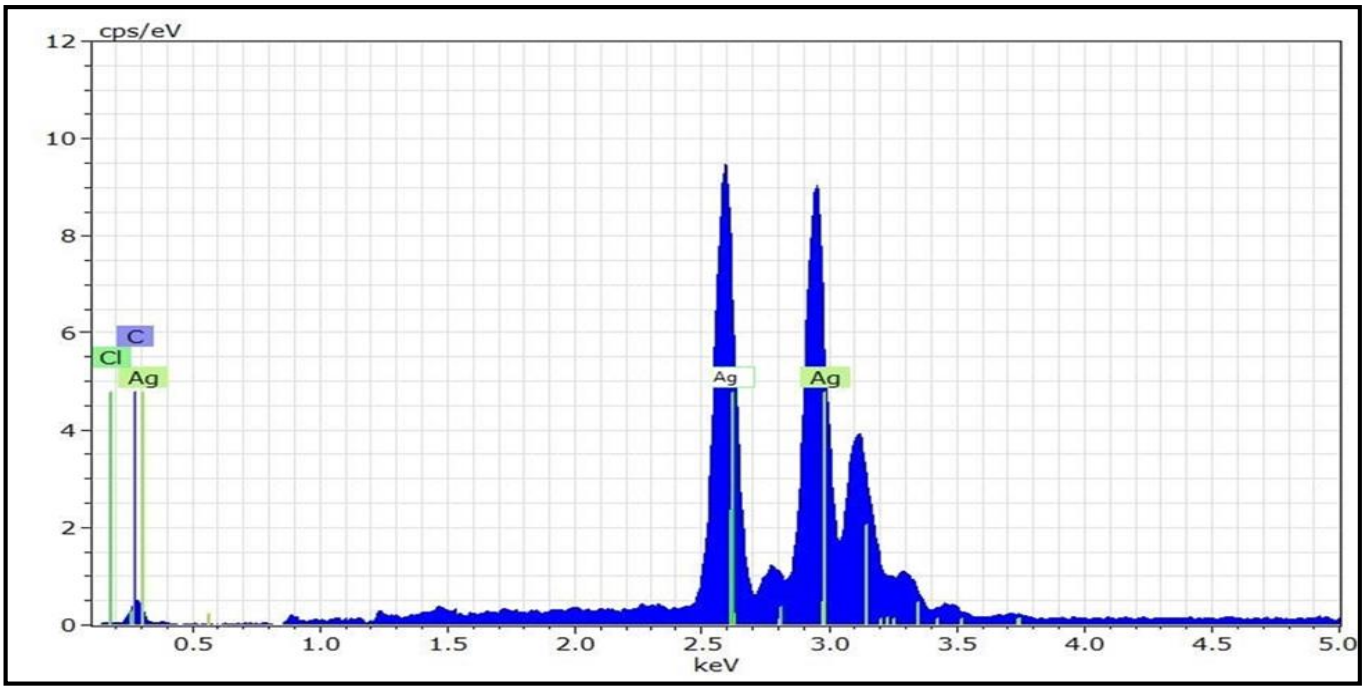

Figure (10): EDS analysis of synthesized Ag NPs

-Scanning electron microscopy of AgNPs

In SEM the sample of Ag NPs found an irregular shape and average size of about 23 nm as shown in Figure (11). Other results disagree with Varadavenkatesan, T.et al [26].

But aggregation made size measurements difficult at 85.77nm [27]. These AgNPs exhibited an elongated morphology due to the aggregation of two or more AgNPs.

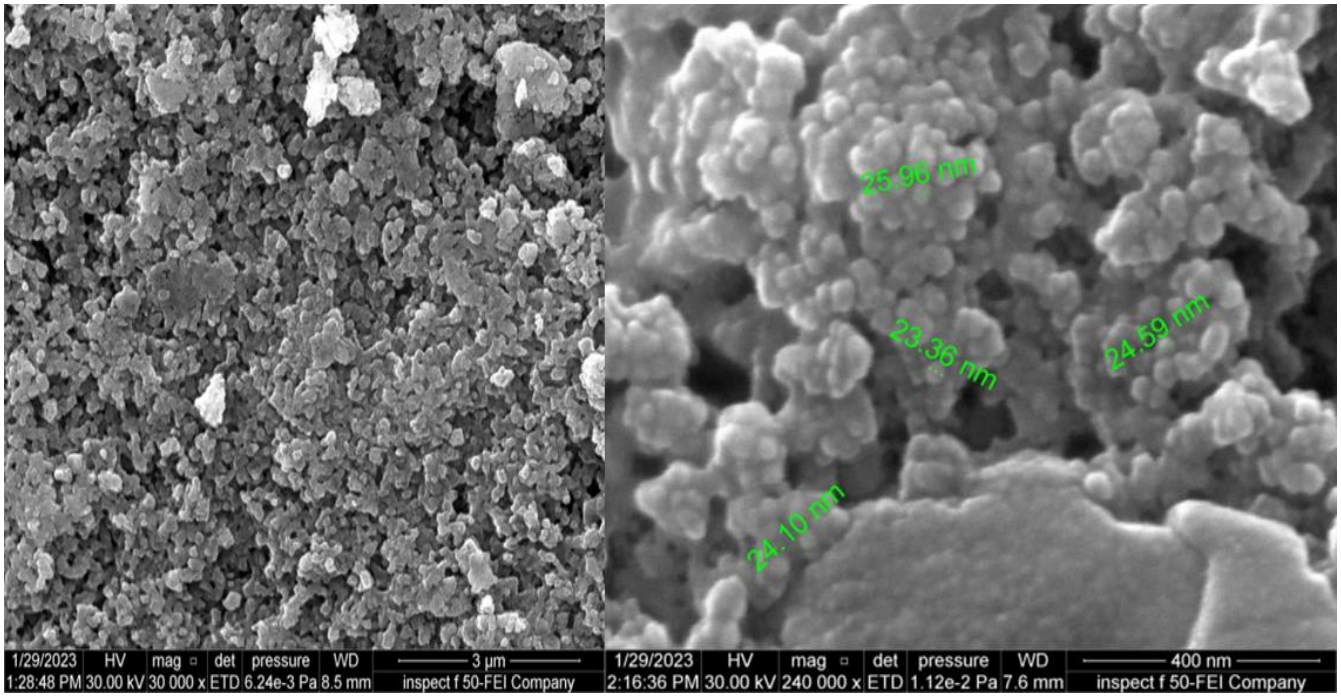

Figure (11): SEM Biological sample of Ag NPs

-Zeta Potential (ZP):

The zeta potential was found to be -29.30 mv for AgNPs as shown in Figure (12)

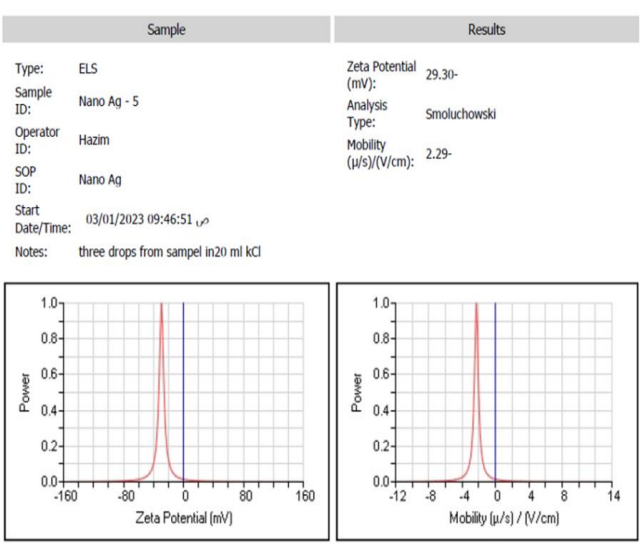

Figure (12): Zeta Potential analysis of synthesized AgNPs

According to [28], zeta potential describes the stability of Nano formulations. Particles smaller than 20 nm have higher mobility, less light scattering, and a narrower concentration spectrum. The zeta potential test is impacted by the lowest concentration used to evaluate particle size because it impacts the particle surface charge.

Antibacterial activities of Ag NPs without magnetic field

The antimicrobial capacity of the prepared Ag NPs was evaluated by a biological method and well diffusion assay against the fourth bacterium S. aureus. After plate incubation, as evidence of antibacterial effectiveness, the diameter of the inhibition zone was found (Table 1). The minimum inhibitory concentration, which was found to be 32 g/ml, was used as the baseline concentration to measure the MIC assay. This concentration showed the best efficacy against resistant strains of Gram-positive and negative bacteria against multidrug-resistant bacteria [29].

Figure (13), Table (1), and the outcome display distribution Mean Zone of Bacterial Inhibition following treatment with various concentrations (4-64) g/mL of AgNPs was significantly different (p 0.05), according to the statistical analysis. With regard to various species of Gram-positive and Gram-negative bacteria, there are notable variances

Table 1. Results for AgNPs effects on bacterial strain without magnetic field

Bacterial Isolate	Mean ± SD Zone of Bacterial Inhibition in mm Treated with Different Concentrations (in µg/mL) of Ag NPs					p Value
	4	8	16	32	64	
S. aureus	5.23±0.2^{a}	8.2±0.21^{b}	9.3±0.3^{c}	10.2±0.3^{d}	11.3±0.16^{e}	<0.0001 **
S. pyogenes	4.3±0.1^{a}	6.2±0.1^{b}	8.3±0.1^{c}	12.3±0.1^{d}	14.4±0.21^{e}	<0.0001 **
Klebsiella Sp.	2.1±0.3^{a}	3.5±0.2^{b}	4.3±0.11^{c}	8.6±0.1^{d}	9.16±0.13^{e}	<0.0001 **
P. aeruginosa	4.26±0.15^{a}	6.18±0.15^{b}	8.2±0.2^{c}	11.3±0.1^{d}	13.3±0.21^{e}	<0.0001 **
E. coli	3.3±0.15^{a}	6.5±0.21^{b}	9.53±0.15^{c}	14.4±0.4^{d}	19.5±0.44^{e}	<0.0001 **
Salmonella	3.17±0.12^{a}	4.3±0.18^{b}	6.17±0.15^{c}	7.2±0.1^{d}	9.1±0.2^{e}	<0.0001 **

Different letters (a, b, c, d, e) consider significant differences at p < 0.05 between groups in a row

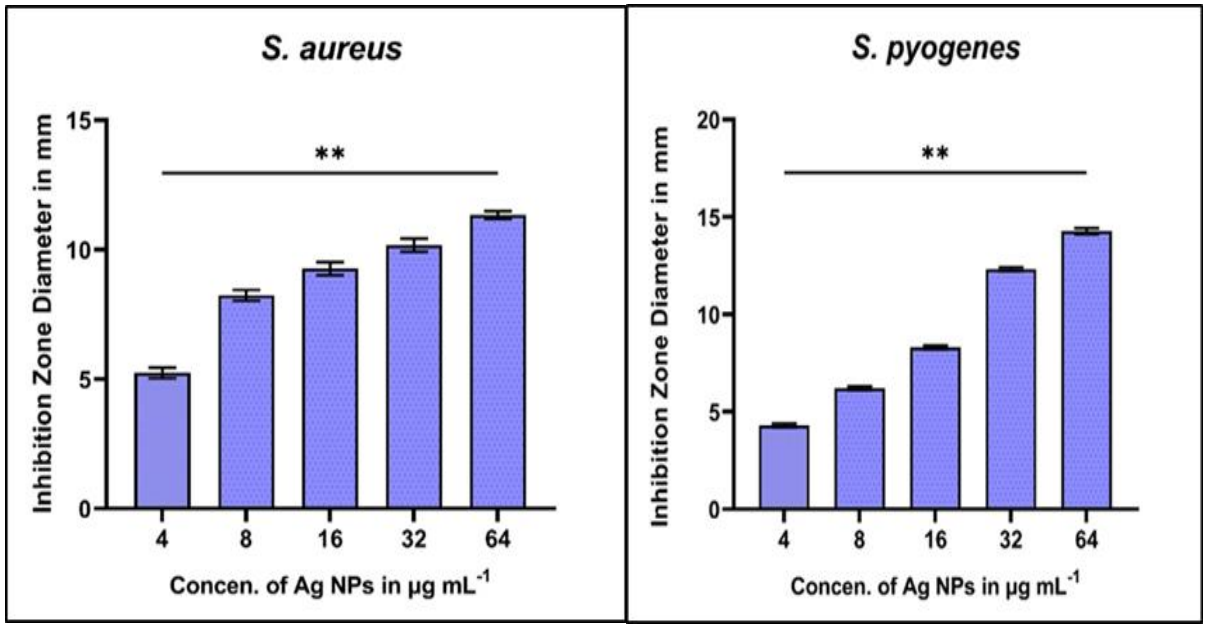

Figure (13): Mean (± SD) Zone of Bacterial Inhibition in mm Treated with Different Concentrations (in µg/mL) of AgNPs against gram-positive bacteria S. aureus and S. pyogenes without Magnetic Field Standard Deviation, (n = 3)

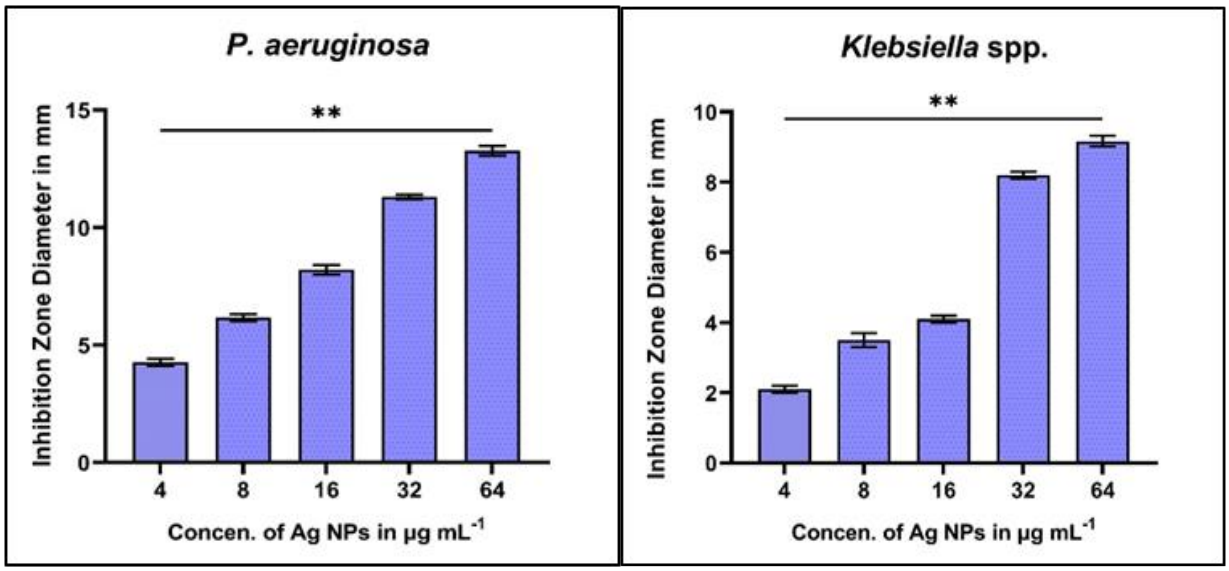

Figure (14) A substantial variation in the distribution Mean Zone of Bacterial Inhibition after Different Concentrations of AgNPs was highlighted by statistical analysis (p 0.05). Where it is possible to notice significant differences against Gram-negative Klebsiella spp and E. coli, compared to other species P. aeruginosa and Salmonella spp the differences were less significant at Different Concentrations.

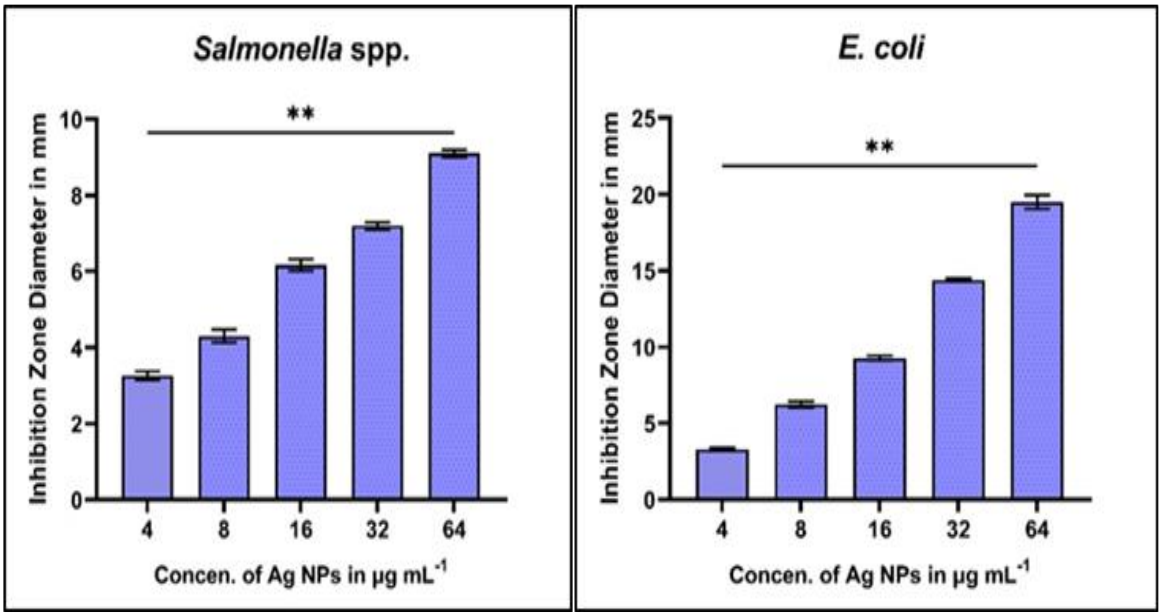

Figure (14): Mean (± SD) Zone of Bacterial Inhibition in mm Treated with Different Concentrations (in µg/mL) of AgNPs against gram-negative bacteria Klebsiella spp, P. aeruginosa, E. coli, and Salmonella spp without Magnetic Field Standard Deviation, (n = 3)
**p < 0.05, NS: Non- Significant, SD: Standard Deviation

Other results of the assay [30] The smaller the AgNPs are, the more quickly they can adhere to microbial membranes and kill pathogens at the cell surface. This has an impact on how nanoparticles affect pathogens. Other evaluations of film results against Staphylococcus aureus compared to other species showed very good zones of inhibition by the nanoparticles.

Antibacterial Activity with the magnetic field

The prepared AgNPs antimicrobial was evaluated for the best inhibitory the minimum inhibitory concentration which is 32µg/ml concentration that was observed without a magnetic field manner as illustrated in the table. By comparison between the results in Table 1 and results in Table 2, we can conclude that the use of astatic magnetic field results in more inhibition zone, demonstrating and confirming the effect of a weak static magnetic field on the antibacterial activity of the synthesized silver nanoparticles [31].

AgNPs were found to have antibacterial action against E. coli in a concentration and time-dependent manner at

a range of low concentrations in the order of 10 M and 100 M [32], which is similar to the current findings. Figure (15) and Table (2) display the outcome. The statistical evaluation highlighted a noteworthy difference. ($p < 0.05$) in the dissemination Mean Zone of Bacterial Inhibition after treated MIC 32 µg/mL of AgNPs with Magnetic Field.

There are significant differences between Gram-negative bacteria with Mean ± SD (9.3±0.1a), (10.2±0.2c), (15.2±0.15d) and (13.3±0.1e) for Salmonella spp., Klebsiella spp., E. coli, and P. aeruginosa respectively, while no significant differences between gram-positive bacteria with Mean ± SD (12.5±0.15b) and (12.53±0.2b) for S. aureus and S. pyogenes respectively

Table (2). Mean (± SD) Zone of Bacterial Inhibition in mm Treated with Different Concentrations (in µg/mL) of AgNPs effects on bacterial with Magnetic Field

Mean ± SD Zone of Bacterial Inhibition in mm Treated with 32 µg/mL of Ag NPs						p Value
Salmonella spp.	S. aureus	S. pyogenes	Klebsiella spp.	E. coli	P. aeruginosa	
9.3±0.1[a]	12.5±0.15[b]	12.53±0.2[b]	10.2±0.2[c]	15.2±0.15[d]	13.3±0.1[e]	<0.0001 **

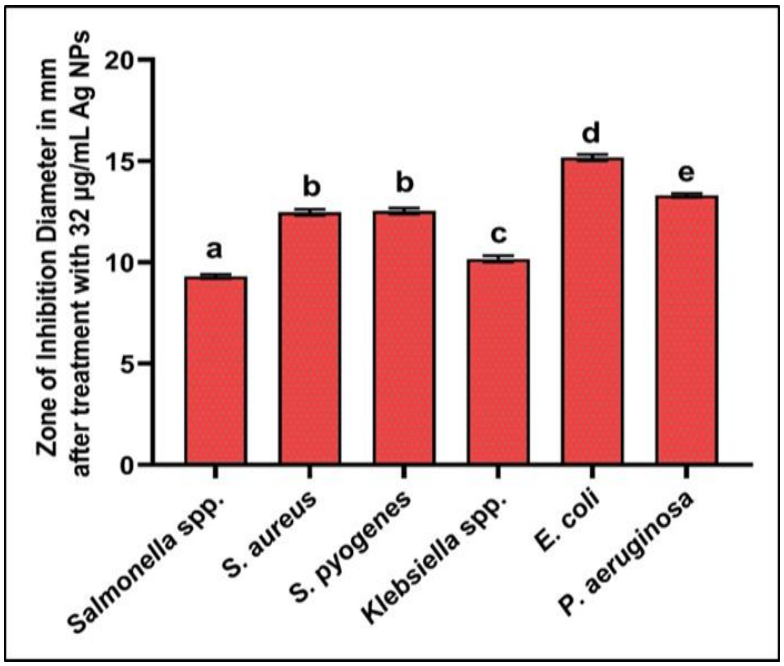

Figure (15): Mean (± SD) Zone of Bacterial Inhibition in mm Treated with (32 µg/mL) of AgNPs Effects on MDR gram-positive and negative bacterial with Magnetic Field

Different letters (a, b, c, d, e) consider significant differences at $p < 0.05$ between groups in a row

Maybe because of the surface charge of AgNPs, according to what was found in the examination of Zeta, it was equal to (-29.30), the silver nanoparticles have a charge, and this charge is affected by the magnetic field, which leads to the emergence of an additional driving force for the movement of nanoparticles according to Lorenz's law(F=qvB), which leads to an increase in the effectiveness of nanoparticles against bacteria

The Cytotoxic Effect of AgNPs on Lymphocytes

The results of the cytotoxicity assays showed that there was no discernible decline in the viability of human lymphocytes treated with the biologically produced AgNPs nanoparticles, indicating that these techniques could be used as an effective replacement for the existing other physical methods used to assess environmental toxicity after interacting with AgNPs for 24 hours, human lymphocytes showed cytotoxicity as measured by MTT tests.

The Silver NPs exhibit a similar significant loss in cellular viability and the lowest reduction in cellular viability at (62.5, 125, 250, 500, and 1000 g/ml). The cellular vitality of human lymphocytes after treatment with AgNPs is illustrated in Table (3) and Figure (16). The outcomes support this. The concentration of AgNPs employed determines how cytotoxic they are to cells. AgNPs were evaluated for their cytotoxicity at various concentrations, and it was discovered that while cell viability was not considerably affected by AgNPs at 50 g/mL, it was significantly decreased in cell lines at 1000 g/mL .

Table (3): Cellular viability in human lymphocytes by MTT assay when treated with AgNPs

Concentration µg/ml	Viability %
1000 µg/ml	69.620
500 µg/ml	66.772
250 µg/ml	66.455
125 µg/ml	61.392
62.5 µg/ml	63.924

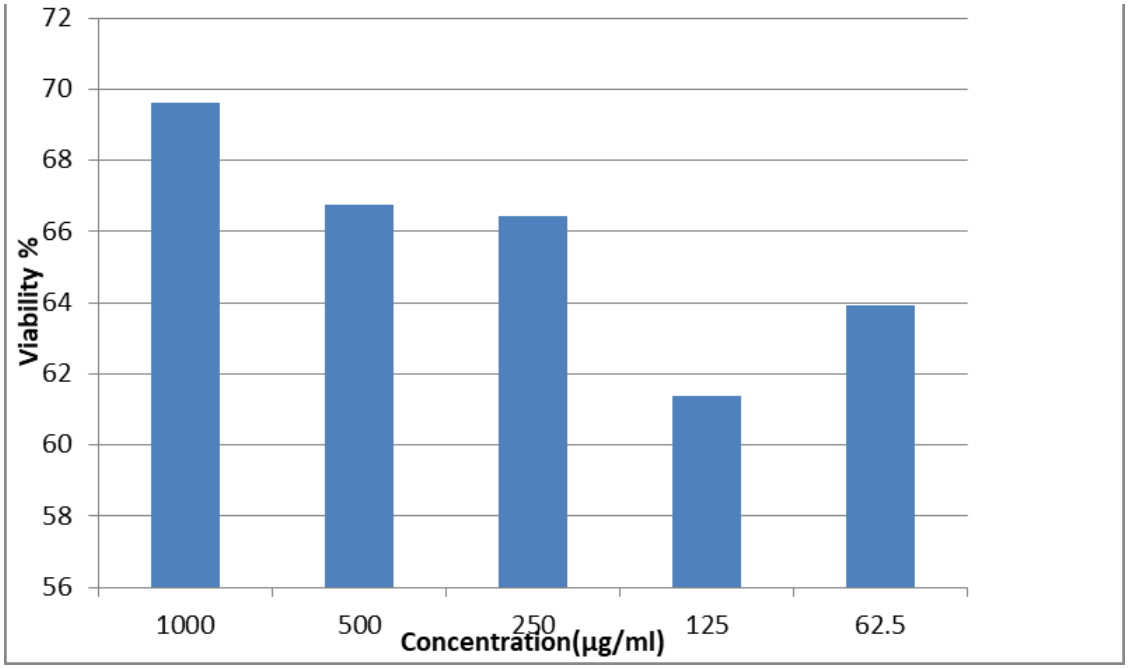

Figure (16): Cellular viability in human lymphocytes by MTT assay when treated with AgNPs

Conclusions

The synthesis of Ag nanoparticles by Biosynthesized method which is used in this research is suitable to prepare Ag nanoparticles in accordance with the size of the particle and homogeneity of the product. the antibacterial activity of the Ag NPs product with a magnetic field is also greater than that seen in the control culture (without a magnetic field) Multi-resistant bacterial strains have created an alarming situation that has encouraged the development of new therapies for infections.

Ag NPs were effectively created using a simple, direct, low-cost, high-yield, and environmentally friendly approach. When tested against several bacterial strains, Ag NPs showed outstanding antimicrobial activity.

References

1. L. S. Mohammed and M. E. Ahmed, "Effects of ZnO NPS on Streptococcus pyogenes in vivo," *Ann Trop Med & Public Health,* vol. 23, p. S452, 2020.
2. C. Remschmidt, C. Schröder, M. Behnke, P. Gastmeier, C. Geffers, and T. S. Kramer, "Continuous increase of vancomycin resistance in enterococci causing nosocomial infections in Germany− 10 years of surveillance," *Antimicrobial Resistance & Infection Control,* vol. 7, pp. 1-7, 2018.
3. T. Togashi *et al.*, "Size-tunable continuous-seed-mediated growth of silver nanoparticles in alkylamine mixture via the stepwise thermal decomposition of silver oxalate," *Chemistry of Materials,* vol. 32, no. 21, pp. 9363-9370, 2020.
4. T. Q. Huy, P. Huyen, A.-T. Le, and M. Tonezzer, "Recent advances of silver nanoparticles in cancer diagnosis and treatment," *Anti-Cancer Agents in Medicinal Chemistry (Formerly Current Medicinal Chemistry-Anti-Cancer Agents),* vol. 20, no. 11, pp. 1276-1287, 2020.
5. A. Hajalilou, L. Ferreira, M. M. Jorge, C. Reis, and M. Cruz, "Superparamagnetic Ag-Fe3O4 composites nanoparticles for magnetic fluid hyperthermia," *Journal of Magnetism and Magnetic Materials,* vol. 537, p. 168242, 2021.
6. A. P. Betancourt, D. Y. Goswami, V. R. Bhethanabotla, and J. N. Kuhn, "Scalable and stable silica-coated silver nanoparticles, produced by electron beam evaporation and rapid thermal annealing, for plasmon-enhanced photocatalysis," *Catalysis Communications,* vol. 149, p. 106213, 2021.
7. H. Righi, J. D. Arruda-Neto, J. G. Gomez, L. F. da Silva, E. S. Somessari, and A. C. Lemos, "Exposure of Deinococcus radiodurans to both static magnetic fields and gamma radiation: observation of cell recuperation effects," *Journal of Biological Physics,* vol. 46, pp. 309-324, 2020.
8. O. Pryshchepa, P. Pomastowski, and B. Buszewski, "Silver nanoparticles: Synthesis, investigation techniques, and properties," *Advances in Colloid and Interface Science,* vol. 284, p. 102246, 2020.
9. S. Singh *et al.*, "Cell extract-containing medium for culture of intracellular fastidious bacteria," *Journal of Clinical Microbiology,* vol. 51, no. 8, pp. 2599-2607, 2013.
10. H. Agarwal, S. Menon, S. V. Kumar, and S. Rajeshkumar, "Mechanistic study on antibacterial action of zinc oxide nanoparticles synthesized using green route," *Chemico-biological interactions,* vol. 286, pp. 60-70, 2018.
11. Z. H. Kadhim, M. E. Ahmed, and I. Şimşek, "The Synergistic Effect of Copper Nanoparticles and Vancomycin in Vitro and in Vivo," *Pakistan Journal of Medical & Health Sciences,* vol. 16, no. 08, pp. 594-594, 2022.
12. J. A. A. Abdullah, L. S. Eddine, B. Abderrhmane, M. Alonso-González, A. Guerrero, and A. Romero, "Green synthesis and characterization of iron oxide nanoparticles by pheonix dactylifera leaf extract and evaluation of their antioxidant activity," *Sustainable Chemistry and Pharmacy,* vol. 17, p. 100280, 2020.
13. M. Cruz-Aponte and J. Caraballo-Cueto, "Balancing fiscal and

mortality impact of COVID-19 mitigation measurements," *Letters in Biomathematics,* vol. 8, no. 1, pp. 255–266, 2021, doi: 10.30707/LiB8.1.1647878866.134162.

14. E. C. o. A. S. Testing, "European Committee for Antimicrobial Susceptibility Testing of the European Society of Clinical Microbiology and Infectious Diseases (ESCMID). Determination of Minimum Inhibitory Concentrations (MICs) of Antibacterial Agents by Broth Dilution," *Clin. Microbiol. Infect,* vol. 9, pp. 1-8, 2003.
15. M. Balouiri, M. Sadiki, and S. K. Ibnsouda, "Methods for in vitro evaluating antimicrobial activity: A review," *Journal of pharmaceutical analysis,* vol. 6, no. 2, pp. 71-79, 2016.
16. P. Skehan *et al.*, "New colorimetric cytotoxicity assay for anticancer-drug screening," *JNCI: Journal of the National Cancer Institute,* vol. 82, no. 13, pp. 1107-1112, 1990.
17. H. Singh, J. Du, P. Singh, and T. H. Yi, "Extracellular synthesis of silver nanoparticles by Pseudomonas sp. THG-LS1. 4 and their antimicrobial application," *Journal of pharmaceutical analysis,* vol. 8, no. 4, pp. 258-264, 2018.
18. E. T. J. Mason *et al.*, "Decoding comparable morphologies: Pigmentation validated for identifying southern California Paralabrax larvae," *FishTaxa,* 2022.
19. A. Abeer Mohammed, M. M. Abd Elhamid, M. K. M. Khalil, A. S. Ali, and R. N. Abbas, "The potential activity of biosynthesized silver nanoparticles of Pseudomonas aeruginosa as an antibacterial agent against multidrug-resistant isolates from intensive care unit and anticancer agent," *Environmental Sciences Europe,* vol. 34, no. 1, pp. 1-15, 2022.
20. M. A. Shaker and M. I. Shaaban, "Synthesis of silver nanoparticles with antimicrobial and anti-adherence activities against multidrug-resistant isolates from Acinetobacter baumannii," *Journal of Taibah University medical sciences,* vol. 12, no. 4, pp. 291-297, 2017.
21. L. Khrema, A. Saad, A. Alnesser, and C. Capapé, "First record of Baillon's wrasse Symphodus bailloni (Labridae) in the Eastern Mediterranean Sea coast of Syria," *FishTaxa-Journal of Fish Taxonomy,* vol. 25, 2022.
22. R. Singh *et al.*, "Synthesis, optimization, and characterization of silver nanoparticles from Acinetobacter calcoaceticus and their enhanced antibacterial activity when combined with antibiotics," *International journal of nanomedicine,* pp. 4277-4290, 2013.
23. M. Kgatshe, O. S. Aremu, L. Katata-Seru, and R. Gopane, "Characterization and antibacterial activity of biosynthesized silver nanoparticles using the ethanolic extract of Pelargonium sidoides DC," *Journal of Nanomaterials,* vol. 2019, pp. 1-10, 2019.
24. C. Demarchi, M. d. Souza, L. S. d. Souza, F. L. Galli, and S. M. Pilati, "Lung histopathological changes in Swiss mice exposed to narghile smoke," *Jornal Brasileiro de Patologia e Medicina Laboratorial,* vol. 58, p. e4442022, 2022.
25. C. Lunardi, A. Gomes, F. Rocha, J. De Tommaso, and G. Patience, "Experimental methods in chemical engineering: Zeta potential," *Canadian Journal of Chemical Engineering,* vol. 99, no. 3, pp. 627-639, 2021.
26. T. V. Varadavenkatesan, R.; Selvaraj, R. , "Green synthesis and structural characterization of silver nanoparticles synthesized using the pod extract of Clitoria ternatea and its application towards dye degradation. Mater. Today Proc," pp. 27–29., 2019.
27. R. B. Domingues, C. A. S. Giafferi, M. V. d. Santos, F. B. V. d. M. Leite, and C. Senne, "Diagnosis of neurosyphilis with cerebrospinal fluid pcr: a systematic review," *Jornal Brasileiro de Patologia e Medicina Laboratorial,* vol. 58, p. e4432022, 2022.
28. S. Hajji *et al.*, "Nanocomposite films based on chitosan–poly (vinyl alcohol) and silver nanoparticles with high antibacterial and antioxidant activities," *Process Safety and Environmental Protection,* vol. 111, pp. 112-121, 2017.
29. B. Sánchez-Alcaraz, V. Jiménez, D. Muñoz, and J. Ramón-Llin, "Effectiveness and distribution of attack strokes to finish the point in professional padel," *Revista Internacional de Medicina y Ciencias de La Actividad Fisica y Del Deporte,* vol. 22, no. 87, pp. 635-648, 2022.
30. I. A. Orlov *et al.*, "New silver nanoparticles induce apoptosis-like process in E. coli and interfere with mammalian copper metabolism," *International Journal of Nanomedicine,* pp. 6561-6574, 2016.
31. D. Chapa-Guadiana, O. Ceballos-Gurrola, G. Gastélum-Cuadras, J. Pérez-García, J. Valadez-Lira, and F. Ochoa-Ahmed, "Dermatoglyphic Profile and Predominant Physical Qualities in Mexican University Athletes: Exploratory Study," *REVISTA INTERNACIONAL DE MEDICINA Y CIENCIAS DE LA ACTIVIDAD FISICA Y DEL DEPORTE,* vol. 22, no. 87, pp. 551-563, 2022.
32. P. Saravana Kumar, C. Balachandran, V. Duraipandiyan, D. Ramasamy, S. Ignacimuthu, and N. A. Al-Dhabi, "Extracellular biosynthesis of silver nanoparticle using Streptomyces sp. 09 PBT 005 and its antibacterial and cytotoxic properties," *Applied Nanoscience,* vol. 5, pp. 169-180, 2015.